Journal of Civil Engineering
The Institution of Engineers, Bangladesh
Vol. CE 24, No. 2, 1996

ECCENTRICALLY LOADED STRIP FOOTING ON A SAND LAYER OVERLYING A RIGID SMOOTH BASE

Md. Zoynul Abedin[1]

ABSTRACT : This paper presents major findings concerning influences on ultimate bearing capacity due to a strip footing having a rough base resting on the surface of a sand layer overlying a smooth rigid base. Model tests for bearing capacity were conducted using sand layers of different thicknesses in a glass sided model tank. The smooth interface condition of the sand layer with the rigid base of the tank was achieved through a rubber membrane grease sandwich system. Plane strain conditions were maintained using lubricated rubber membranes on the side walls of the tank. A mechanical sand spreader was used to form the sand bed layer of uniform density. The relative density and hence the triaxial friction angle of the bed was maintained constant. Specially prepared load cells were used at the base of the model footing to measure the stresses while vertical load was applied to the footing at a desired eccentricity using a strain controlled loading rig. Stereo-photogrammetric technique, which essentially uses still photographs, was used to study the kinematics of the sand layer. Results of model tests were indicative of a maximum layer thickness after which the deformation behaviour of the sand mass was found to change and bearing capacity became constant. Thickness and eccentricity factors were introduced in the generalised bearing capacity formula. The study of the kinematics of the sand mas gave a reasonable explanation of the influences of these factors on ultimate bearing capacity of a sand layer.

KEY WORDS: Bearing capacity, Strip footing, Eccentric load, Finite sand layer, Rigid base, Smooth interface.

INTRODUCTION

The actual behaviour of soil when subjected to external forces is a complex problem due to its formation variability in nature. The modern theoretical investigation started with the simplest case of homogeneous, isotropic medium of semi-infinite extent with strip loading. Considering the above assumptions, several investigators presented their theories on various aspects of foundation behaviour, particularly of the failure mechanism and hence the bearing capacity.

To consider the stability of the structures investigators presumed that the centre of loading coincided with the centre of the foundation. However, the consideration of economy and often the existence of adjacent construction necessitate the use of other types of loading, for example, eccentric and/or inclined loads. In the foremost method of solving this problem, the conception of a neutral axis at the centre of a loaded beam was used to compute the stresses beneath a foundation due to eccentric loading, more commonly known as conventional analysis. The

1 Department of Civil Engineering, BUET, Dhaka-1000, Bangladesh

effect of eccentric loading on a foundation was initially studied by Meyerhof (1953) in which he introduced the concept of effective width. Of the other important theoretical contributions, mention can be made of Prakash and Saran (1971).

From the practical point of view, it is not always safe and economic to design a foundation considering semi-infinite layer beneath it when there exists a finite layer. This necessitated a more realistic approach to the solution of the problem. The early pioneers in this field were Burmister (1945), Livneh (1965), Vyalov (1967), Milovic et. al. (1970) and Mandel and Salencon (1972). However, their theories involve various assumptions concerning soil strength and weight and the interface condition of the soil with the underlying stratum.

Though a significant volume of experimental investigation has been reported in the literature on different aspects of foundation behaviour, particularly using semi-infinite layer, detailed experimental or theoretical works are yet to be reported for the case of finite layer thickness and eccentric loading especially using smooth soil stratum interface condition. Thus, the present research was aimed to investigate the effects of load eccentricity and layer thickness on bearing capacity and kinematics of the soil mass with particular reference to smooth interface condition.

Any experimental investigation can be carried out either in the laboratory using models or in the field on the actual foundation. Technical and economic difficulties prohibit the use of field tests due to the difficulty in obtaining the required layer thicknesses in the field and the uncertainly about the interface condition. Laboratory model tests are economic and reliable since the soil characteristics and model dimensions can be chosen so that the required parameters can be studied. The performance of the actual foundation in this case may be predicted if similarity laws are maintained.

In order to achieve the objectives of the present research a sophisticated experimental system was developed for the purpose in which a spreader was designed to deposit sand in a model tank forming a uniform sand bed. An instrumented footing containing load cells at the base was used to measure the induced stresses. Load was applied to the footing using a strain controlled loading rig through two loading blades. The side walls of the tank were lubricated using silicon grease and rubber membranes. These membranes were also used to trace the displacement fields of sand mass in the stereophotogrammetric technique. The smooth rigid stratum interface condition was achieved using a grease membrane sandwich system.

The effects of load eccentricity and layer thickness on bearing capacity were studied by introducing eccentricity and layer thickness factors. A design chart is proposed, which considers the combined effect of these factors.

THE EXPERIMENTAL SYSTEM

The experimental system consisted mainly of a tank, a sand spreader, a loading rig, an instrumented footing, displacement measuring transducers and a data recording system. The displacement

field within the soil mass was measured using the stereo-photogrammetric technique as suggested by Andrawes (1976). The experimental system is outlined briefly as under and details can be found in Abedin (1986).

The sand used in the investigation was Loch Aline sand of Scotland. It is a white coloured fine to medium sand with particle size distribution as shown in Fig.1. The specific gravity of the sand was 2.64. The maximum and minimum porosities were 34% and 45% respectively. The porosity - φ_t relationship of the sand was determined carrying out triaxial compression tests on 100 mm diameter samples at a strain rate of 0.10 mm/min. A constant porosity of sand of 35% (δ_d =1y 16.9 kN/m^3, I_D = 88%) was used throughout the research programme. In order to obtain the desired porosity, the sand was circulated through a hopper gap of the sand spreader from a precalibrated height. The triaxial friction angle of the sand at bed condition porosity was determined as 36.5°.

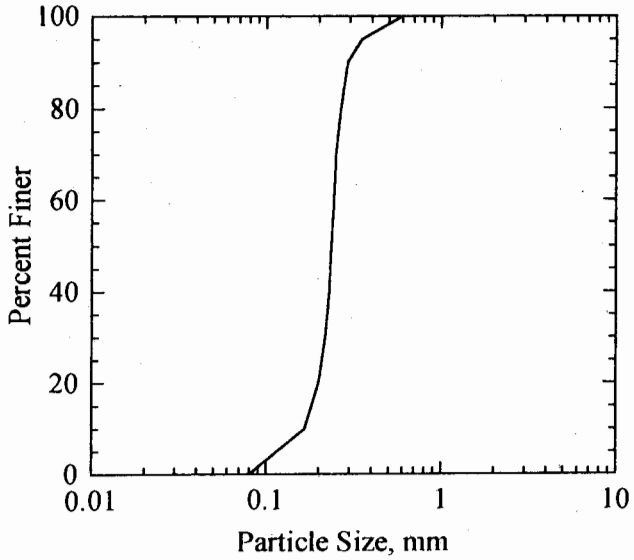

Fig 1. Particle Size Distribution of Loch Aline Sand

The tank was used as a sand bed container. The skeleton of the tank consisted of four side frames and a base frame, all were made of M.S. angles and bars. The frames were connected to each other by bolting and welding. The internal dimensions of the tank were 120 mm x 1908 mm x 100 mm. The shorter opposite sides were bounded by 25 mm thick plywood planks, and the longer sides by 18 mm thick glass plates to facilitate photographic works. The tank base was covered with M.S. plates.

The sand spreader used for the deposition of sand in the tank was similar to that described by Whitaker (1967). The most important feature of the sand spreader was a movable steel hopper. The horizontal forward and backward movement of the hopper over the tank was controlled by an electric motor through an endless chain. The rotation of a solid steel roller mounted at the base of the hopper causes a constant flow of sand curtain through a gap between the roller and the top adjustable plate.

An apparatus consisting mainly of a steel frame and an aluminum plate was used to level off the sand layer. It was used to remove the surcharge developed due to penetration of footing into sand layer during loading. A depth gauge was fabricated to measure the thickness of the deposited sand layer.

A strip footing constructed of steel plates and having base dimensions of 120 mm x 900 mm was used in the investigation. The height of this hollow footing was 200 mm. Two similar sets of four V-shaped grooves were provided on the upper face of the base plate to provide the knife edged blades with proper seats at different eccentricities during loading. A single load cell block (Block 1) was fixed along the base at one edge of the footing to measure the normal and shear stresses. A second block of 4 medium sized load cells (Block 2) and a third one (Block 3) containing 13 small cells were installed near to the mid length of the footing. Similar to that of load cell in Block 1, Block 2 cells also measure the normal and shear stresses while the Block 3 cells were used to measure the contact vertical stress thus to show its distribution along the footing width. A schematic diagram of the footing and load cell arrangement are shown in Fig. 2. Rough base of the footing was achieved by gluing B.S. grade S2, grit No. 40 glass paper on to the footing base. The friction angle between sand and glass paper was measured to be 34°. The normal load capacity for large and small cells were 10 kN and 1.75 kN respectively. The shear load capacities for the corresponding cells were 2.5 kN and 0.5 kN. All the load cells were made from a solid block of aluminum alloy (HE15W, E = 70×10^6 kN/m^2) and contains either horizontal or both horizontal and vertical webs, where strain gauges were fixed and connected to electrical circuits, designed to be sensitive to either normal or both normal and shear loads respectively. All the load cells were calibrated several times during the testing programme.

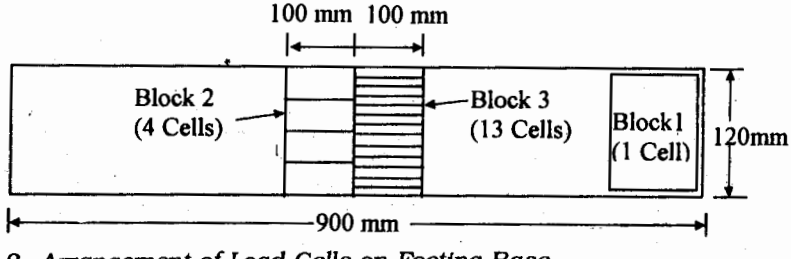

Fig 2. Arrangement of Load Cells on Footing Base

A strain controlled loading rig was used to load the footing. The loading mechanism was composed of an electrical motor to drive down a mechanical jack. The jack was connected to a moving bridge with two loading bars. A pair of knife edged loading blades were attached to the bars to transfer the load onto the footing. The rig was mountable at different positions on the top of the tank. A 50 kN capacity load cell was placed inside a cylindrical housing situated between the jack and the moving bridge of the rig. A speed regulator was used to control the vertical displacement rate from 0 to 90 mm/hr. A displacement rate of 5 mm/hr was applied during loading of the footing. Two LVDT's (Linear Variable Displacement Transducer) and a mechanical dial gauge were used to measure the vertical displacements of the footing. A Solatron data logger consisting of a Data Transfer Unit, an Analog Scanner and a Digital Volt Meter was used to record the data of load cells and transducers.

In order to achieve the smooth interface condition the surface of the tank bed (stratum bed) was first polished using fine grained metallic paper. A clean rubber membrane of size equal to the stratum bed area was placed over a wooden board. Smaller membrane strips were greased and placed over the previous one, with a 10 mm overlap between the adjacent strips. This grease membrane sandwich system was then placed over the tank bed. Before pouring the sand into the tank, the glass plates of the tank were cleaned with acetone and grids of 50 mm squares were drawn on the inner surface of the front glass wall. On a large number of small rubber membranes mainly of three sizes, 120 mm x 100 mm, 60 mm x 100 mm and 60 mm x 50 mm, random dots were marked with permanent black ink. The membranes were greased and stuck to the glass plate. These were used to facilitate stereo-photogrammetry. A schematic diagram of grease membrane arrangements are shown in Fig. 3.

A camera (Minolta X-300) loaded with a slide film (Kodak, Ecktacromme) was placed on a tripod over a fixed position approximately 1.5 m from the side wall of the tank. Photographs were taken, at a regular interval of approximately 10 minutes, of the dotted membranes during loading. Qualitative vertical and horizontal displacements were obtained using three dimensional stereo view of the slide photographs and the principles of sterephotogrammetry (Andrawes, 1976). In this method a relief map of the displacement field can be visualised, while any two slide films are viewed through a 3-D viewer, depending on the direction of the movement of sand mass.

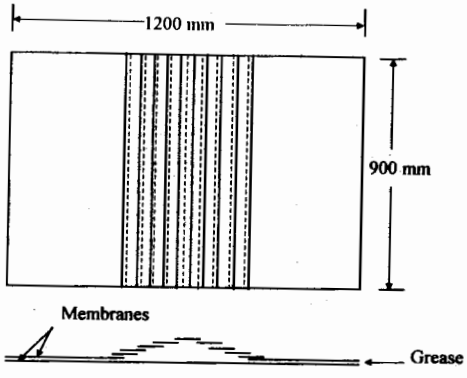

(a) Grease Membrane Sandwich at Stratum Base

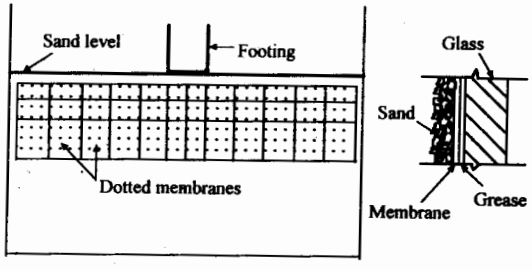

(b) Typical Arrangement of Membranes on Side Walls

Fig 3. Arrangement of Lubrication Systems

TEST PROGRAMME, RESULTS AND DISCUSSION

In total a number of 17 tests for bearing capacity were performed. Tests were conducted with load eccentricities as a ratio to the width of the footing (e/B) of 0, 1/12, 1/6, 1/3. The layer thickness, H, was maintained at H/B ratios of 0, 0.5, 1.0, 1.5, 3.0, 3.5. Load Q was measured from the average readings of all the load cell blocks in the footing. The terminologies for the physical quantities used in the present investigation are defined in Fig. 4. In order to examine the reproducibility of the results some of the tests were repeated. Through out the test programme, an average initial porosity of the sand was maintained at 35% (corresponding to ϕ_t = 36.5°). In explaining the test results an adjustment factor of 1.1 as suggested by Lee (1970) was used to estimate the plane strain angle of sand from its triaxial value.

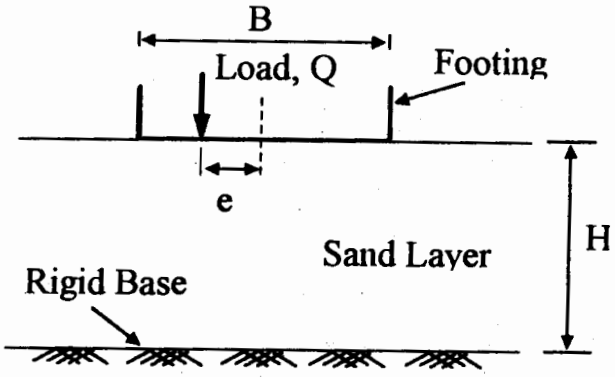

Fig 4. Definitions of B, e. H and Q

ULTIMATE BEARING CAPACITY OF SAND

The ultimate load and thus the average vertical stress beneath the footing was determined from the readings of both cylindrical cell at the loading rig and the cantilever cells at the footing base. The LVDT's gave the settlements of footing at loading point. The stress settlement relationships were thus obtained. In almost all the tests a distinct drop was noticed after the peak load had been reached. In other cases, the ultimate bearing capacity was considered at the point at which the slope of the stress settlement curve reached zero at a point of steady minimum slope. The results of ultimate bearing capacity and corresponding settlement are presented in Table 1.

Table 1. Ultimate Bearing Capacity and Settlement

H/B	Bearing capacity for different e/B (kN/m^2)				Settlement at ultimate load for different e/B, (mm)			
	e/B=0	e/B=1/12	e/B=1/6	e/B=1/3	e/B=0	e/B=1/12	e/B=1/6	e/B=1/3
0.50	18.83	10.40	10.26	7.43	2.57	9.65	2.00	1.89
1.00	19.19	-	13.79	12.48	2.53	-	1.64	3.34
1.50	28.58	-	20.37	13.69	3.43	-	2.38	1.60
3.00	48.65	-	25.19	12.33	8.20	-	4.20	4.39
3.50	48.85	29.90	22.61	12.73	-	5.86	2.94	1.45

The variations of ultimate bearing capacity with layer thickness for different eccentricities are shown in Fig. 5. In general, for relative layer thickness, H/B > 0.5 to a limiting value the bearing capacity was found to decrease with the increasing eccentricity and decreasing relative layer thickness. The limiting layer thickness also showed a trend with the load eccentricity, a higher value at a lower eccentricity. For the eccentricities 0, B/6 and B/3 the limiting values of H/B were approximately 3.0, 2.0 and 1.5 respectively. Though similar trend was observed in case of eccentricity of B/12, comments on the value of limiting thickness could not made for the lack of sufficient data.

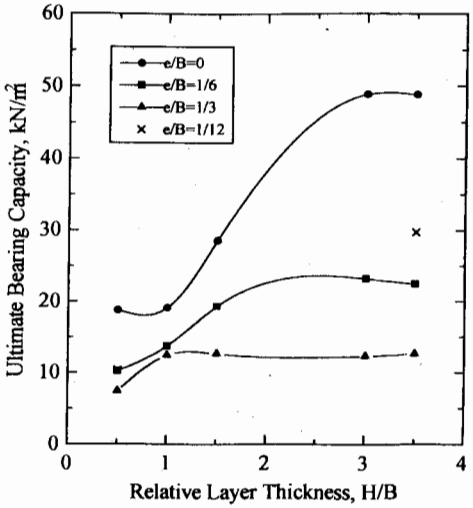

Fig 5. Variation of Ultimate Bearing Capacity with H/B

The variation of bearing capacity with both layer thickness and eccentricity may be explained by examing the displacement field of sand mass in stereo pictures. It was observed, from stereo pictures, that for a layer thickness less than the limiting value the failure in the soil mass was caused due to splitting of the layer and sliding at the stratum surface after the formation of dense core beneath the footing. For thicker layers the failure was initiated along a curved surface above the stratum base rather than by splitting. A typical qualitative expression of displacement fields are shown in Fig. 6. Here the length of arrows describes the qualitative displacement. Details can be found in Abedin (1986).

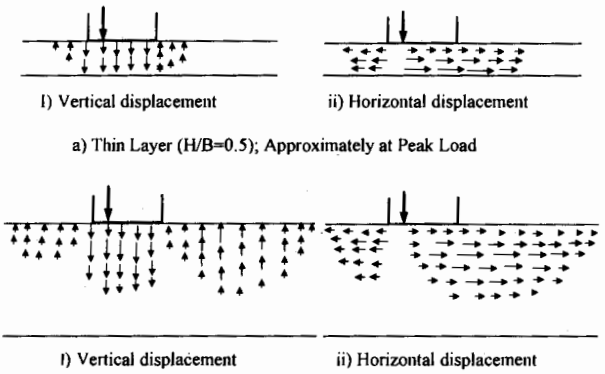

Fig 6. A Qualitative Displacement Field of Sand Mass

Thus for a thin layer the bearing capacity appeared to be a function of earth pressure, the magnitude of which was found to vary with layer thickness. In case of thick layer (H/B > limiting thickness) the frictional properties of the stratum surface had no influence and the problem was found to be similar to that of semi infinite layer.

As far as the eccentricity is concerned, it was visualised from the stereo pictures that the edge of the footing started losing contact with the soil on the application of eccentric load. The higher was the eccentricity, the larger was the contact free area and smaller was the peak load. These variations of bearing capacity can be seen in Fig. 5.

As there exists no previous experimental or theoretical work on the eccentrically loaded footing resting on a sand over a smooth rigid interface, direct comparison of the experimental results was not possible. However, in Fig. 7 a comparison is made with the existing theories concerning eccentric load and semi infinite layers. The theories of Meyerhof (1953), Prakash and Saran (1971) and conventional theory of linear stress distribution were considered. The values of $Q_{u(eccen)}/Q_{u(cen)}$, where $Q_{u(ecce)}$ and $Q_{u(cen)}$ denotes total ultimate load per unit length of the footing for eccentric and concentric positions respectively, were compared.

The experimental results had a reasonable agreement with the theories when H/B > 3.0, particularly for smaller eccentricities up to B/6. However, for higher eccentricities the results showed better agreement with the conventional theory.

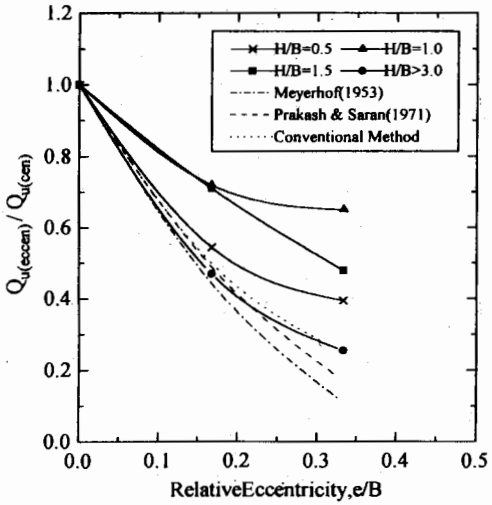

Fig 7. Experimental and Predicted Load Ratios

BEARING CAPACITY, LOAD ECCENTRICITY AND LAYER THICKNESS FACTORS

The following relationship was used to define the ultimate bearing capacity, q_u of a strip footing resting on a layer of soil and subjected to eccentric loading.

$$q_u = 0.5B\gamma F_{\gamma cs} F_{\gamma ts} N_\gamma \quad (1)$$

where $F_{\gamma cs}$ and $F_{\gamma ts}$ are the factors proposed to be used in conjunction with the general bearing capacity factor N_γ to take account for load eccentricity and layer thickness respectively δ is the unit weight of sand.

In calculating the experimental value of N_γ, ultimate bearing capacity of centrally loaded footing with H/B > 3.0 was considered as there was no effect of layer thickness in this range. The values of N_γ proposed by various investigators as a percentage of experimental values are shown in Table 2. It was observed that N_γ showed a close agreement with the predictions of Terzaghi (1943), Meyerhof (1953), Sokolovoski (1965) and Br. Hansen (1961). The experimental results indicated an overestimation of the values on N_γ given by Caquot and Kerisel (1953), Feda (1961) and Vesic (1973).

Table 2. Observed and Predicted Values on N_γ ($\phi_t = 36.5°$, B = 120 mm)

Observed value	(Predicted value/ Experimental value) in Percent						
	Terzaghi (1943)	Meyer-hof (1951)	Caquot & Kerisel (1953)	Br. Hansen (1961)	Feda (1961)	Sokolovoski (1965)	Vesic (1973)
159	105	100	133	108	189	97	126

To examine the effects of eccentricity and layer thickness, the principle of superposition was assumed to be valid i.e. the influence of eccentricity on bearing capacity for a particular layer thickness was independent of the influence of layer thickness itself. As there observed no influence of layer thickness on bearing capacity when H/B is equal to or greater than 3.0, the thickness factor $F_{\gamma ts}$ was assumed to be 1.0 in this range. The eccentricity factor for N_γ ($F_{\gamma es}$) was calculated by using the ultimate bearing capacity results with H/B > 3.0 in Eq. (1). The eccentricity factors for all eccentricities at this thickness were determined and assumed to valid for all the layer thicknesses. The thickness factors, $F_{\gamma ts}$, were then calculated taking the ultimate bearing capacity values from Fig. 5 and the eccentricity factor values. The eccentricity and thickness factors are presented in Table 3. Both these factors were found to decrease with increasing eccentricity. The eccentricity factors are compared with the results of other investigators in Fig. 8. For smaller eccentricities (e/B < 1/6) the values of $F_{\gamma es}$ were in close agreement with Meyerhof (1953) and Prakash and Saran (1971), whereas, for larger eccentricities the conventional theory was found to give good results.

Table 3. Eccentricity and Thickness Factors (Strip Footing, Smooth Interface)

e/B	$F_{\gamma es}$	Thicknes Factor, $F_{\gamma ts}$				
		H/B=0.50	H/B=1.00	H/B=1.50	H/B=2.00	H/B>3.00
0	1.00	0.37	0.39	0.58	0.76	1.00
1/12	0.61	0.38	-	-	-	1.00
1/6	0.47	0.40	0.61	0.86	0.97	1.00
1/3	0.25	0.61	0.88	1.00	1.00	1.00

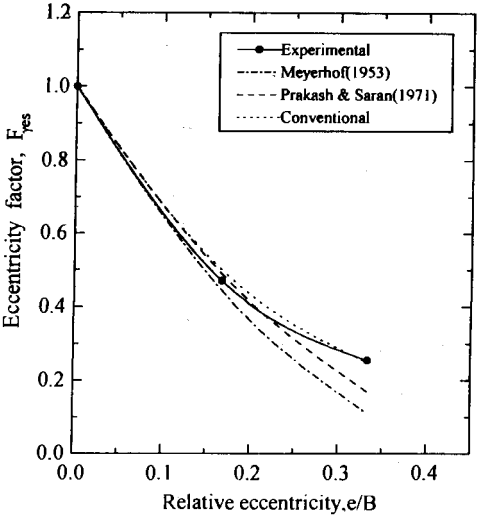

Fig 8. Experimental and Predicted Eccentricity Factors

The thickness factors are presented as a function of H/B and e/B respectively in Figs. 9 and 10. Fig. 9 shows that for a particular load eccentricity the thickness factor $F_{\gamma ts}$ decreases with decreasing layer thickness. The factor increases with increasing eccentricity for a particular layer thickness, Fig 10, depicting that for a larger load eccentricity the influence of layer thickness is likely to be less.

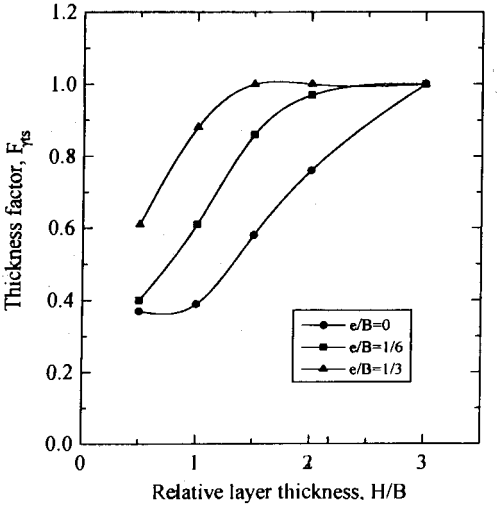

Fig 9. Thickness Factors for Different Eccentricities

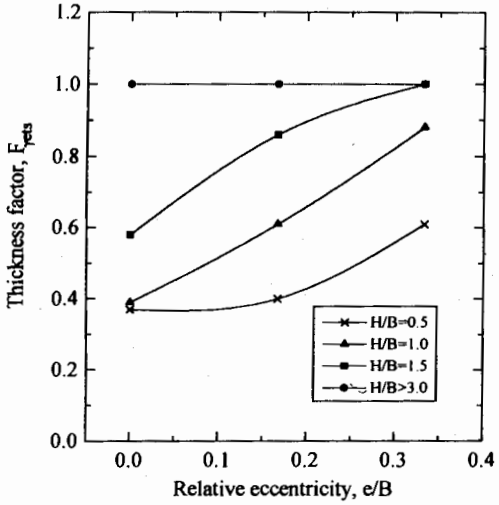

Fig 10. Variation of Thickness Factor with Load Eccentricity

DESIGN CHARTS FOR COMBINED ECCENTRICITY AND THICKNESS FACTORS

From design point of view, it is always desirable that the effect of these factors should be obtained from a simple diagram. The combined eccentricity and thickness factor was thus introduced in the present study. The combined factor (multiplier of N_γ) is denoted as $F_{\gamma ets}$ which is numerically equal to the product of $F_{\gamma es}$ and $F_{\gamma ts}$. It is proposed as a design chart to be used to account for the combined effect of load eccentricity and layer thickness in calculating the bearing capacity of a strip footing on a sand layer underlain by a smooth rigid base. The chart is presented in Fig. 11 as a contour of $F_{\gamma ets}$ with relative eccentricity (e/B) and relative layer thickness (H/B).

CONCLUSIONS

The study described in this paper was aimed at investigating the effects of load eccentricity and layer thickness on the behaviour of a strip footing resting on a sand layer underlain by a smooth surfaced horizontal rigid base. The following important conclusions and suggestions can be made from the observations.

i) The ultimate bearing capacity remains constant beyond a limiting layer thickness. This limiting thickness depends on degree of load eccentricity, For eccentricities 0, B/6 and B/3 the limiting thicknesses are respectively, 3.0, 2.0, and 1.5 times the width of footing.

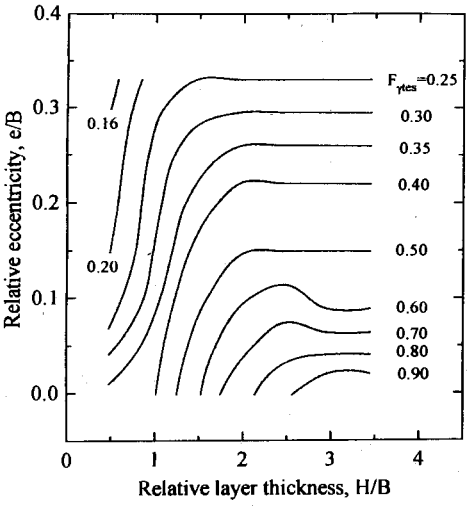

Fig 11. Design Chart for Combined Eccentricity and Thickness Factor ($F_{\gamma ets}$)

ii) The general bearing capacity formula may be modified by introducing load eccentricity and layer thickness factors ($F_{\gamma es}$ and $F_{\gamma es}$ respectively) along with N_γ as its multipliers.

iii) The theories of Meyerhof (1953), Prakash and Saran (1971) provide a reasonable account for the load eccentricity up to B/6. For larger eccentricities the cnventional theory gives a better prediction of ultimate bearing capacity.

iv) The thickness factor, $F_{\gamma ts}$ increases with increasing layer thickness upto a limiting value for a given eccentricity. The factor, in general, increases with increasing eccentricity.

v) The values of general bearing capacity factor N_γ (ϕt = 36.5°) given by Meyerhof (1953) and Sokolovoski (1965) give excellent prediction of ultimate bearing capacity for a centrally loaded footing on a semi infinite layer (H/B > 3.0)

vi) Fig 11 may be used as a design chart to estimate the combined eccentricity and thickness factor ($F_{\gamma ets}$). However, its generalisation requires further study taking triaxial friction angle as a variable.

REFERENCES

Abedin, M.Z. (1986), Eccentrically Loaded Strip Footing on a Sand Layer Overlying a Rigid Stratum, Ph.D. thesis, University of Strathclyde, Glasgow, U.K.

Andrawes, K.Z. (1976), The Use of Stereophotogrammetry for Measuring Displacement Fields, Report, Science Research Council, U.K.

Br. Hansen, J. (1961), "A General Formula for Bearing Capacity", Bulletin 11, Denish Geotechnical Institute, 38-454, Copenhagen.

Br. Hansen, J. (1970), "A Revised and Extended Formula for Bearing Capacity", Bulletin 28. Denish Geotechnical Institute, 5-11, Copenhagen.

Burmister, D.M. (1945), The General Theory of Stresses and Displacements in Layered System - 1, Jnl. of Applied Physics, Vol 16, 89-127.

Caquot, A. and Kerisel, J. (1953), "Ultimate Bearing Capacity of a Foundation Lying on the Surface of a Cohesionless Soil", Proc., 3rd ICSMFE, Vol. 1, 336-339, Switzerland.

Feda, J. (1961), "Research of the Bearing Capacity of Lose Soil", Proc 5th ICSMFE, Vol. 1, 635-642, Paris.

Lee, K.L. (1970), "Comparison of Plane Strain and Triaxial Tests on Sand", Proc. ASCE. JSMED, Vol. 96, 901-923.

Livneh, M. (1965), "The Theoretical Bearing Capacity of Soils on a Rock Foundation", Proc., 6th ICSMFE, Vol. 2, 122-126.

Mandel, J. and Salencon, J. (1972), "Force Portante d'un sol sur une Assise Rigide (etude theorique)", Geotechnique 22, No., 1, 79-93.

Meyerhof, G.G. (1953), "The Bearing Capacity of Foundations Under Eccentric and Inclined Loads", Proc 3rd ICSMFE, Vol, 1. 440-445, Switzerland.

Milovic, D.M. Touzot, G. and Tournier, J.P. (1970). "Stresses and Displacements in an Elastic Layer due to Inclined and Eccentric Load over a Rigid Strip", Geotechnique, 20, No. 3, 231-252.

Prakash, S and Saran, S. (1971), "Bearing Capacity of Eccentrically Loaded Footing", Proc. ASCE, JSMFED, SMI, 95-117.

Sokolovoski, V.V. (1965), Statics of Granular Media, Pergamon Press, London.

Terzaghi, K. (1943), Theoretical Soil Mechanics, John Wiley & sonn, New York.

Vesic, A.S. (1973), "Analysis of Ultimate Loads of Shallow Foundations", Proc. ASCE. JSMFED, Vol. 99, 45-73.

Vyalov, S.S. (1967), "Bearing Capacity of Weak Soil Layer with Underling Rigid Base", Proc., 3rd Asian Regional Conf. on SM & FE, 245-247, Haifa.

NOTATION

B	Width of footing
E	Young's modulus of elasticity
e	Eccentricity of load
H	Thickness of sand layer
$F_{\gamma es}$	Load eccentricity factor for smooth interface
$F_{\gamma ts}$	Layer thickness factor for smooth interface
$F_{\gamma ets}$	Combined eccentricity and thickness factor for smooth interface
I_D	Density index or relative density
N_γ	Bearing capacity factor semi infinite layer
Q	Applied load on the footing
Q_u	Ultimate or peak load on the footing
q_u	Ultimate bearing capacity
$q_{u(eccen)}$	Ultimate bearing capacity due to eccentric loading
$q_{u(cen)}$	Ultimate bearing capacity due to central loading
ϕ_t	Triaxial friction angle of sand
γ	Unit weight of sand
γ_d	Dry unit weight of sand